ROMANIAN JOURNAL OF INFORMATION SCIENCE AND TECHNOLOGY
Volume 28, Number 2, 2025, 173–184
doi: 10.59277/ROMJIST.2025.2.05

Separation of Different Orbital Angular Momentum Photon States with Log-pol Transformation

George Andrei BULZAN[1,2,*], Roxana REBIGAN[1], Mihai KUSKO[1], Rebeca TUDOR[1] and Cristian KUSKO[1]

[1]National Institute for Research and Development in Microtechnologies IMT, 077190 Bucharest, Romania
[2]Faculty of Physics, University of Bucharest, P.O. Box MG-11, Bucharest-Măgurele, Romania
Email: george.bulzan@imt.ro*, roxana.rebigan@imt.ro, mihai.kusko@imt.ro, rebeca.tudor@imt.ro, cristian.kusko@imt.ro
* Corresponding author

Abstract. An optical vortex undergoing a logarithmic – polar transformation is unwrapped from a ring – like shape to a straight line segment whose tilt is determined by the order of the vortex. Due to this property, components with continuous optical surface performing logarithmic – polar transformation are employed for the optical vortices sorting as a function of their orders. In this work we show that a logarithmic – polar component with its optical surface approximated by four discrete levels performs with a good approximation the same transformation of the optical vortices.

Key-words: Fourier terms; log-pol transformation.

1. Introduction

Optical vortices (OVs) are diffraction patterns presenting a helicoidal wavefront in which the photon has an orbital angular momentum (OAM) that is equal to $m\hbar$ where m is the order of the OV and $\hbar$ is the reduced Plank constant [1]. Their configuration is quite peculiar consisting on a donut-like shape with a hole in its center for $m \neq 0$. In the center point of an OV the phase is not defined.

Due to the fact that the OAM of an OV is easily adjustable and the fact that the OAM can form an infinite Hilbert space, OVs have a wide range of applications in different domains. For instance, OAM can be used for coding and transmitting information in classical and quantum level [2]. Thus, the modulation of information in a photon's OAM leads to a significant increase of the information capacity of the communication channels [3,4]. Also, it was proven that OAM can be used in quantum key distribution (QKD) scenarios with high security [5] and in different quantum communication protocols [6]. For reasons concerning these domains of applications of OVs it is very important to have efficient methods of separating different OAM states.

One of the simplest ways to achieve this task is to use fork-like holograms [7]. However, this works only for a small number of OAM and has a limited efficiency. Other proposed methods are the interferometric ones where i.e. Mach-Zender interferometers with Dove prisms on their arms [8] or interferometers based on Fourier and inverse Fourier gates [9] are used. Another approach, which is the subject of this work, is by performing a logarithmic-polar (log-pol) transformation with the use of aspherical lens of focal distance f whose phase function is described by this transformation. These lens together with a phase corrector will be able to change the OV's donut-like shape into a linear one whose tilt depends on the OAM. Thus, we create a correspondence between the OAM and the optical path [10–13].

In this work we will perform a log-pol transformation by using optical elements whose surface are discretized in 4-levels. This will allow us to Fourier expand the phase function of those components. The higher terms will eventually be ignored because they are small. The numerical results will be compared with the experimental ones.

2. Theoretical Background

The log-pol transformation consists of converting from the cartesian coordinates to the logarithmic-polar coordinates defined by [2]:

$$u = -a \ln \frac{\sqrt{x^2+y^2}}{b} \tag{1}$$

$$v = a \arctan \frac{y}{x}, \tag{2}$$

where $a = \frac{d}{2\pi}$ and b are scaling and positioning parameters. It was shown by G. Ruffato and H. Kobayashi [14] that this transformation can be performed by an optical component with the following phase function:

$$\phi_1(x,y) = \frac{ka}{f}\left(y \arctan \frac{y}{x} - x \ln \frac{\sqrt{x^2+y^2}}{b} + x - \frac{x^2+y^2}{2a}\right), \tag{3}$$

where $k = \frac{2\pi}{\lambda}$ is the wave number and λ is the wavelength. Here we added an extra term due to the sphericity of the lens of focal distance f. Thus, the integral of diffraction becomes:

$$u_{m,n}(x,y,z) = \frac{\lambda}{iz}\int_{-\infty}^{\infty}\int_{-\infty}^{\infty} dx_0 dy_0 u_{0,m,n}(x_0,y_0) e^{\frac{ik}{2z}((x-x_0)^2+(y-y_0)^2)+i\phi_1(x_0,y_0)}. \tag{4}$$

For simplicity we will consider in this study that the OVs have a Laguerre-Gaussian form. This means that [15]:

$$u_{0,m,n} = \left(\frac{\sqrt{x^2+y^2}}{w_0}\right)^n e^{im \arctan \frac{y}{x}}, \tag{5}$$

where w_0 is the initial waist of the beam from which we obtain the OV's and n is a quantum number associated to LGOV's.

In the following, we will show that by preforming a Fourier expansion of a phase function corresponding to an aspherical component with the optical surface discretized in 2^N levels, one finds that the leading term is equal to the phase function for the component with the continuous surface. The higher order terms of the Fourier expansion bring their own contribution in the diffraction integral.

As the number of levels increases the contribution of the higher order terms becomes smaller such that in the limit of large N the discreet optical surface approximates very well to the continuous one. To illustrate this, we present, as an example, the Fourier expansion of a spiral phase plate (SPP) generating OV, whose optical surface is discretized in 2^N levels. Its phase function is:

$$e^{i\Phi(\phi)} = \begin{cases} 1, 0 < \phi \leq \frac{\pi}{M2^{N-1}} \\ e^{\frac{i\pi}{M2^{N-1}}}, \frac{\pi}{M2^{N-1}} < \phi \leq \frac{\pi}{M2^{N-2}} \\ \ldots \\ e^{i\pi\frac{2^N-1}{2^{N-1}}}, \pi\frac{2^N-1}{2^{N-1}M} < \phi \leq \frac{2\pi}{M}, \end{cases} \tag{6}$$

where $M = m \pm m_{SPP}$, m is the order of the OV and m_{SPP} is the order of the SPP. Knowing that this function has the period $\frac{2\pi}{M}$ we Fourier expand it and get:

$$e^{i\Phi(\phi)} = \sum_{n=1}^{\infty} a_n \cos(nM\phi) + b_n \sin(nM\phi), \tag{7}$$

where

$$a_n = \frac{M}{\pi}\int_0^{\frac{2\pi}{M}} e^{i\Phi(\phi)} \cos(nM\phi)d\phi = \begin{cases} \frac{2^N \sin\frac{\pi}{2^N}}{\pi(q2^N+1)} e^{-\frac{i\pi}{2^N}}, \textit{for } n = 1 + q2^N, q \in Z \\ \frac{2^N \sin\frac{\pi}{2^N}}{\pi(q2^N-1)} e^{-\frac{i\pi}{2^N}}, \textit{for } n = -1 + q2^N, q \in Z \\ 0, \textit{ else,} \end{cases} \tag{8}$$

and

$$b_n = \frac{M}{\pi}\int_0^{\frac{2\pi}{M}} e^{i\Phi(\phi)} \sin(nM\phi)d\phi = \begin{cases} -\frac{2^N \sin\frac{\pi}{2^N}}{i\pi(q2^N+1)} e^{-\frac{i\pi}{2^N}}, \textit{for } n = 1 + q2^N, q \in Z \\ -\frac{2^N \sin\frac{\pi}{2^N}}{i\pi(q2^N-1)} e^{-\frac{i\pi}{2^N}}, \textit{for } n = -1 + q2^N, q \in Z \\ 0, \textit{ else.} \end{cases} \tag{9}$$

We substitute the equations (8) and (9) into the equation (7) and get:

$$e^{i\Phi(\phi)} = \frac{2^N \sin\frac{\pi}{2^N} e^{-\frac{i\pi}{2^N}}}{\pi} \sum_{q=0}^{\infty} \frac{e^{iM\phi(q2^N+1)}}{q2^N+1} - \frac{e^{-iM\phi(q2^N+2^N-1)}}{q2^N+2^N-1}. \tag{10}$$

This result tells us that if one diffracts an OV of order m on a SPP of order m_{SPP} with 2^N levels one gets a superposition of OVs of orders $M, -M(2^N-1), M(2^N+1), M(2*2^N-$

$1), M(2 * 2^N + 1), ...$ In order to get the phase function for a SPP with a continuous surface ($N \to \infty$) we will rewrite the equation (10) as follows:

$$e^{i\Phi(\phi)} = \frac{2^N \sin\frac{\pi}{2^N} e^{-\frac{i\pi}{2^N}+iM\phi}}{\pi} \left(1 + \sum_{q=0}^{\infty} \frac{-2\cos(C_q M\phi)}{C_q^2+1} + i\sum_{q=0}^{\infty} \frac{2C_q \sin(C_q M\phi)}{C_q^2-1}\right), \quad (11)$$

where:

$$C_q = 2^N(q+1). \quad (12)$$

The first infinite sum of the equation can be proven to go to 0 as $N \to \infty$ by using the squeeze theorem. The second infinite sum goes to 0 as well because it is the derivative of the first one with respect to ϕ divided by M. Thus we have:

$$\lim_{N\to\infty} e^{i\Phi(\phi)} = e^{iM\phi} \quad (13)$$

The Fresnel diffractive integral becomes:

$$u_{m,n}(x,y,z) = \frac{\lambda}{iz}\int_{-\infty}^{\infty}\int_{-\infty}^{\infty} dx_0 dy_0 \left(\frac{\sqrt{x_0^2+y_0^2}}{w_0}\right)^n e^{\frac{ik}{2z}((x-x_0)^2+(y-y_0)^2)+i\phi_1(x_0,y_0)+iM\phi}, \quad (14)$$

where $\phi = \arctan\frac{y_0}{x_0}$.

In the following, we present the same calculations for an optical component performing the log-pol transformation. More specifically, we will consider a lens with 4-level discretized surface that performs the log-pol transformation. Its phase function can be written as:

$$e^{i\Psi(\phi_1(r,\theta))} = \frac{\cos(\phi_1(r,\theta))}{|\cos(\phi_1(r,\theta))|} + i\frac{\sin(\phi_1(r,\theta))}{|\sin(\phi_1(r,\theta))|}. \quad (15)$$

By Fourier expanding it one gets:

$$e^{i\Psi(\phi_1(r,\theta))} = \frac{4}{\pi}\sum_{q=0}^{\infty} \frac{e^{i\phi_1(4q+1)}}{4q+1} - \frac{e^{-i\phi_1(4q+3)}}{4q+3}, \quad (16)$$

which is quite similar to the equation (10) for $N = 2$ and $M = 1$ but we have the phase ϕ_1 instead of ϕ, the only difference being the factor behind the sum. Thus, the Fresnel integral becomes:

$$u_{m,n}(x,y,z) = \frac{\lambda}{iz}\int_{-\infty}^{\infty}\int_{-\infty}^{\infty} dx_0 dy_0 \left(\frac{\sqrt{x_0^2+y_0^2}}{w_0}\right)^n e^{\frac{ik}{2z}((x-x_0)^2+(y-y_0)^2)+i\Psi(\phi_1(x_0,y_0))+iM\phi}, \quad (17)$$

where $\phi = \arctan\frac{y_0}{x_0}$. We plug eq. (16) into this, make the change from cartesian coordinates to polar coordinates and get:

$$u_{m,n}(\rho,\phi,z) = \frac{8e^{\frac{ikr^2}{2z}}}{izk}\sum_{q=0}^{\infty}\int_0^{\infty}\int_0^{2\pi} d\theta dr \frac{r^{n+1}}{w_0^n}\frac{(-1)^q}{2q+1} e^{\frac{ik}{2z}(\rho^2 - r\rho cos(\phi-\theta))+i(2q+1)\phi_1(r,\theta)+iM\theta}, \quad (18)$$

where the additional phase $\phi_1(r,\theta)$ in this coordinates takes the form:

$$\phi_1(r,\theta) = \frac{ka}{f}\left(r\theta\sin\theta - r\cos\theta\ln\frac{r}{eb} - \frac{r^2}{2a}\right). \tag{19}$$

One can notice that the first term of the sumation in the last equation ($q = 0$) is exactly the optical field obtained by diffracting an LGOV of quantum numbers n and m multiplied by $\frac{4}{\pi}$. Its other terms have a significant contribution that generates background noise around the OV. Another thing worth noticing is that the bigger the rank q of the term is the lesser is its contribution in the sumation. That means that one can take into account only the first 3 terms leading to the following approximation:

$$u_{m,n}(\rho,\phi,z) \approx \frac{8e^{\frac{ikr^2}{2z}}}{izk}\sum_{q=0}^{3}\int_0^{\infty}\int_0^{2\pi} d\theta dr \frac{r^{n+1}}{w_0^n}\frac{(-1)^q}{2q+1}e^{\frac{ik}{2z}(\rho^2 - r\rho\cos(\phi-\theta)) + i(2q+1)\phi_1(r,\theta) + iM\theta}. \tag{20}$$

In Fig. 1 it is shown through some numerical results that the log-pol transformation gradually changes the shape of the OVs of order m = n = 1 formed from the LG beams from their donut-like shape into a linear one as one approaches the focal point of the lens. On the right hand side we have the OV projected on a lens with a 4-level discretized surface and on the left hand side the lens has a continuous surface. At the distance $z = f/4$ as shown in the Fig. 1a and 1d the OVs have an annular shape with a cut on the vertical axis. As one gets closer to the focal point at the distance $z = f/2$ the shape begins to stretch itself to look like a U reversed. At the focal point the OVs' shapes have now become linear. Another thing worth to be noticed is that the projection on 4-level discretized surfaces brings a lot of background noise rendering the OV obtained more unclear. The lesser the value of z the more unclear the OV is. However the shape of the OV is similar to the case in which the OV is projected on a continuous surface.

The Fig. 2 represents numerically OVs of order m = n = 2 projected on lenses with continuous surfaces and with 4-level discretized surfaces. The values of z for which the OV is plotted are $3f/8$, $f/2$ and f . The same observations regarding the transformation of the shape of OV with the distance and the blurriness of the Fig. obtained by projecting on the lens with the discontinuous surface (Fig. 2d, 2e and 2f) as in the precedent situation can be made. The main differences between the OVs of order m = n = 2 and those of order m = n = 1 are the radius of the OV and the length of the linear shape in the focal point both being smaller at the latter.

Finally, the OVs of order m = n = 4 are plotted in Fig. 3. The values of z for which they were plotted are the same as in the previous case. The same observations concerning the change of the shape as z increases and the blurriness of the results obtained through projection on the lens with 4-level discretised surface can be drawn. Also, the dimensions of OVs of this order are bigger than those of order 1 and 2 regardless of the value of z. The values that were chosen here for the scaling and positioning parameters are d = 5 and b = 6mm. Those results are represented in cartesian coordinates.

3. Experimental Setup

In order to experimentally show that indeed a four level log – pol optical component performs within a good approximation the same transformation as a log – pol element with continuous

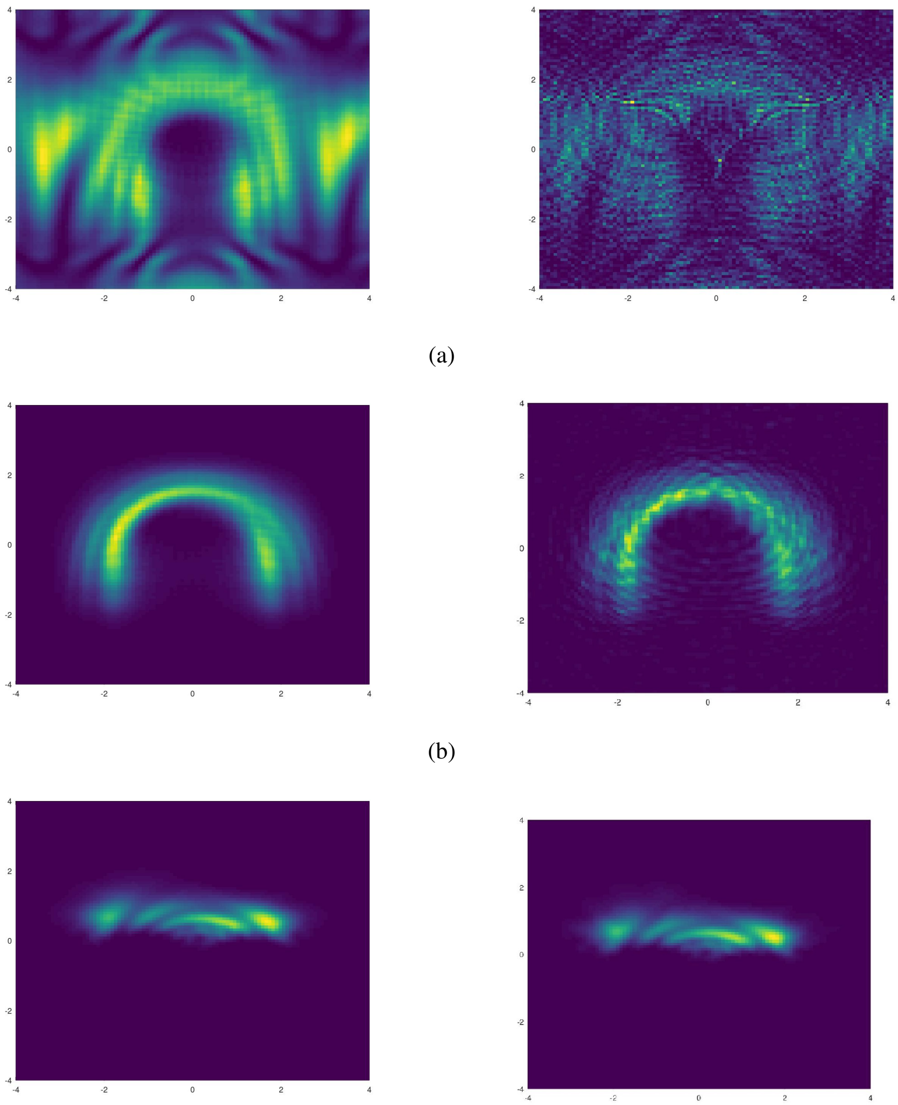

(a) (d)

(b) (e)

(c) (f)

Fig. 1. The numerical result of a LG beam with $OAM = \hbar$ and (n = m) projected on a lens with continuous surface on the left hand side and 4-level discretized surface on the right hand side that performs the log-pol transformation with a focal distance of f = 4000mm at distance a) and d) $z = f/4$, b) and e) $z = f/2$, c) and f) $z = f$ and initial waist $w_0 = 3mm$

optical surface we used a space light modulator (SLM). The experimental setup is illustrated in

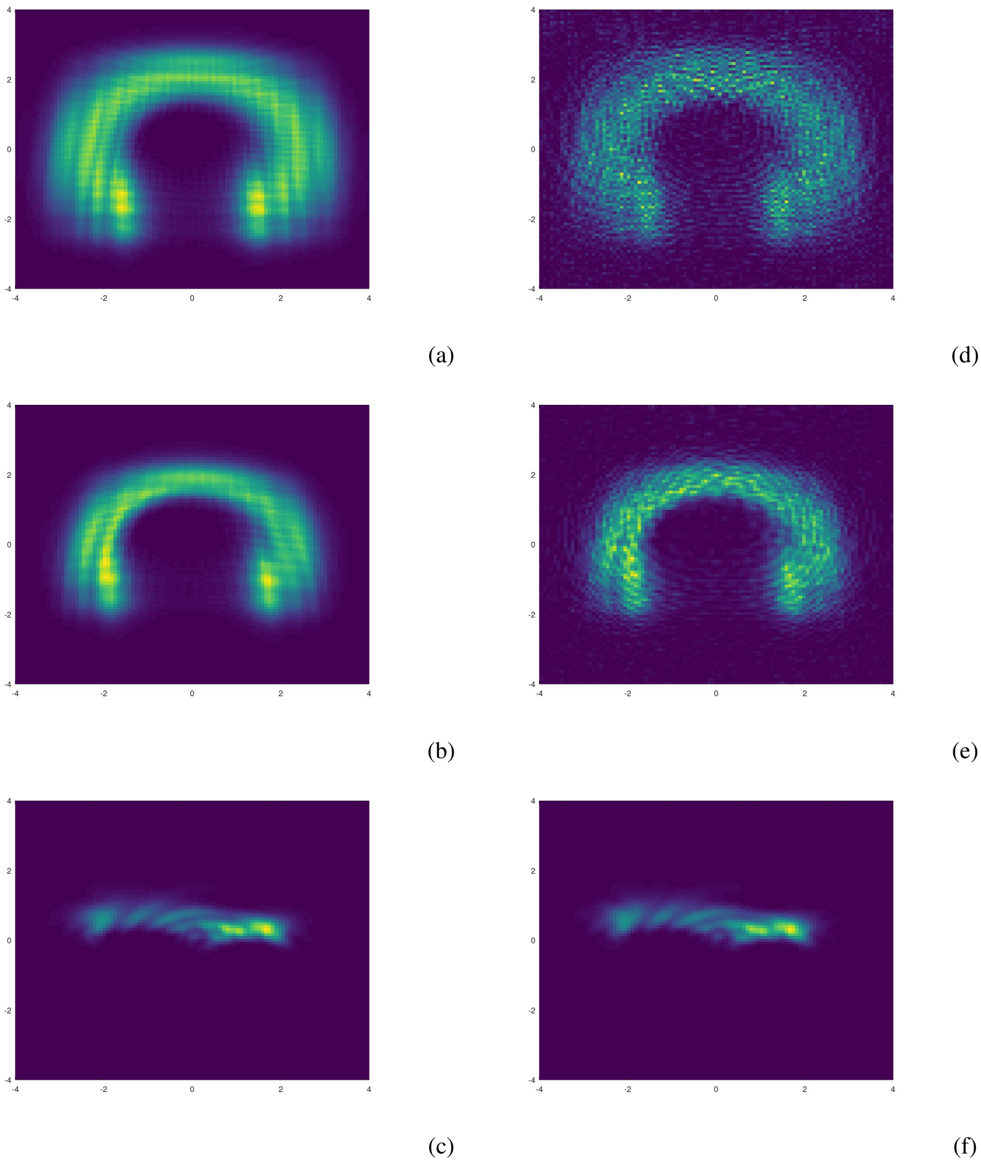

Fig. 2. The numerical result of a LG beam with $OAM = 2\hbar$ and (n = m) projected on a lens with continuous surface on the left hand side and 4-level discretized surface on the right hand side that performs the log-pol transformation with a focal distance of f = 4000mm at distance a) and d) $z = 3f/8$, b) and e) $z = f/2$, c) and f) $z = f$ and initial waist $w_0 = 3mm$

Fig. 4. Here, on the active area of the SLM we transferred a composite image shown in Fig. 5 consisting of two halves. On the right hand side it is transferred the phase function of a spiral

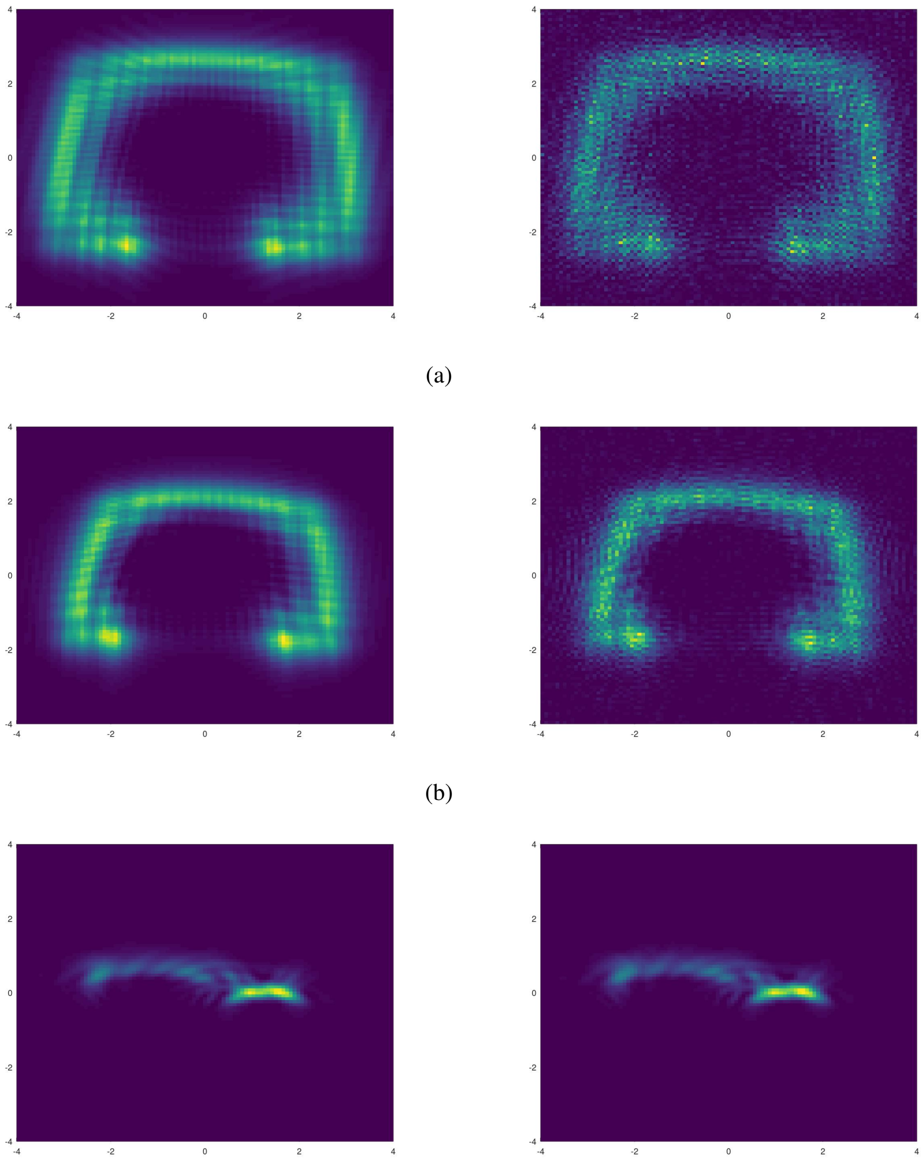

(a) (d)

(b) (e)

(c) (f)

Fig. 3. The numerical result of a LG beam with $OAM = 4\hbar$ and (n = m) projected on a lens with continuous surface on the left hand side and 4-level discretized surface on the right hand side that performs the log-pol transformation with a focal distance of f = 4000mm at distance a) and d) $z = 3f/8$, b) and e) $z = f/2$, c) and f) $z = f$ and initial waist $w_0 = 3mm$.

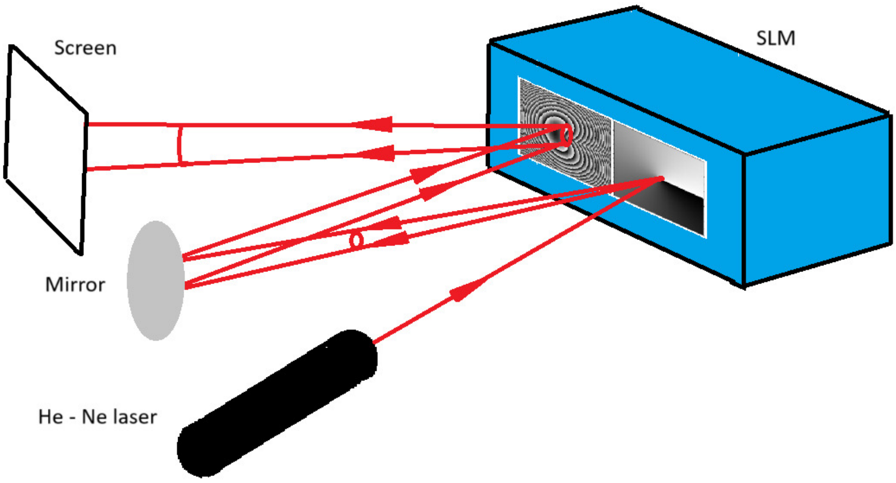

Fig. 4. The experimental setup.

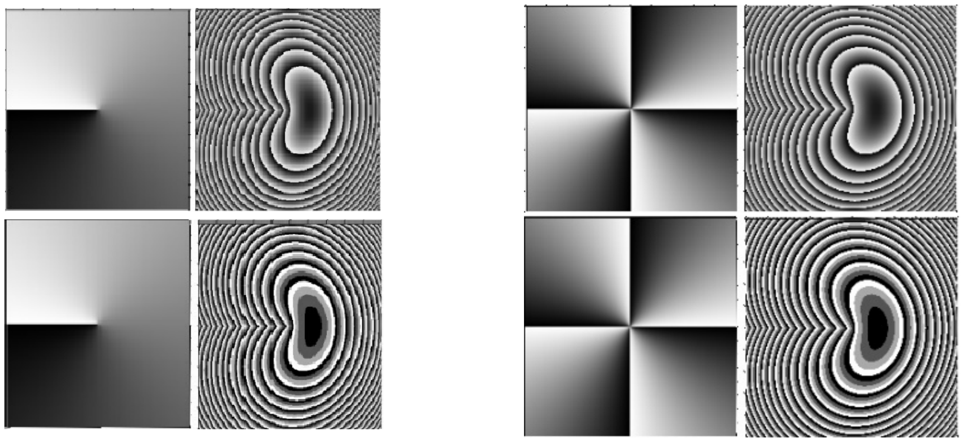

(a) (b)

Fig. 5. The figures used to produce the log-pol transformation. On the left hand side we have the SPP that creates an OV of a)$OAM = \hbar$ b) $OAM = 4\hbar$ and on the right hand side we have the holograms of the log-pol transformation. Upper we have the continuous form of the hologram and lower we have the 4-level discreet form. Those figures were also presented in [16].

phase plate generating a vortex of the order 1 and 4, respectively, and on the left hand side, it transferred the phase function of a log – pol element. The principle of the experimental set – up is straightforward. A Gaussian beam produced by a He – Ne laser with $\lambda = 635nm$ impinges on the right - hand side of the active area of the SLM. The beam is diffracted and converted to an optical vortex of order 1 (or 4). This vortex propagates 500 mm into free space and is reflected towards the left hand side of the active area of the SLM where the log – pol phase function is transferred. The vortex is unwrapped by the log – pol element and propagates until it is projected on a screen whose distance z from the SLM is variable. The diffraction images projected on the screen are recorded with a digital camera at the following propagation distances z=f/4, z=f/2 and z=f. The experiments were performed for the case where the phase function of the log – pol transformation is continuous and for the case where this was discretized in four levels as it is shown in Fig. 5.

3.1. Results

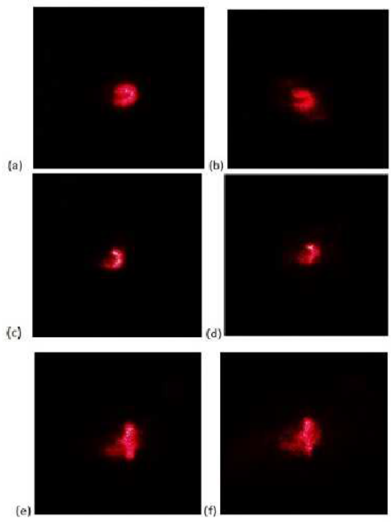

Fig. 6. The experimental results for an OV with $OAM = \hbar$ projected on the log-pol lens with continuous surface (the left hand side) and 4 level discretized level (the right hand side). The propagation distances are z = f/4 for a) and d), z = f/2 for b) and e) and z = f for c) and f). Those results have also been presented in [16].

The experimental results are presented in the Fig. 6 and 7, respectively.

It can be seen the close similarity between the results obtained by the numerical computation of the diffraction integral and the experimental results. Also, the images generated by continuous log – pol component and the discrete one are similar for all practical purposes, fact which indicates the possibility of using 4 level elements for vortices detection applications.

4. Conclusions

In this work, we showed theoretically, numerically and experimentally that an optical component with an optical surface discretized in four levels can perform a log – pol transformation. The optical pattern generated by an optical vortex diffracted by the log – pol component with four level is similar to the one generated by a log – pol component with a continuous surface. This is due to the fact that to the leading term of the Fourier expansion of the phase function corresponding to the four level log – pol component is identical to the one of the phase function corresponding to a continuous surface log – pol optical element. The numerical calculations and

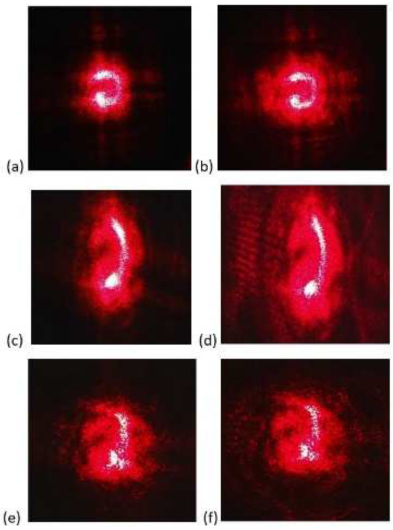

Fig. 7. The experimental results for an OV with $OAM = 4\hbar$ projected on the log-pol lens with continuous surface (the left hand side) and 4 level discretized level (the right hand side). The propagation distances are z = f/4 for a) and d), z = f/2 for b) and e) and z = f for c) and f). Those results have also been presented in [16].

the experiment demonstrate that the contribution to the diffraction integral of the higher order Fourier terms is negligeable. This findings show that one can significantly reduce the technological overhead in the process of manufacturing these log – pol optical components.

Acknowledgement. This research was funded by the European Commission, under Horizon Europe Programme, grant agreement No. 101046651—"4D Microscopy of biological materials by short pulse terahertz sources (MIMOSA)

References

[1] L. ALLEN, S. M. BARNETT and M. J. PADGETT, *Optical Angular Momentum*, CRC Press, 1st Edition, 2016.

[2] M. J. PADGETT, *Orbital angular momentum 25 years on*, Optics Express **25**, 2017, pp. 11265–11274.

[3] J. WANG, J.-Y. YANG, I. M. FAZAL, N. AHMED, Y. YAN, H. HUANG, Y. REN, Y. YUE, S. DOLINAR, M. TUR and E. WILLNER, *Terabit free-space data transmission employing orbital angular momentum multiplexing,* Nature Photonics **6**(7), 2012, pp. 488–496.

[4] G. RUFFATO, M. MASSARI, G. PARISI, and F. ROMANATO, *Test of mode-division multiplexing and demultiplexing in free-space with diffractive transformation optics*, Optics Express **25**(7), 2017, pp. 7859–7868.

[5] M. MIRHOSSEINI, O. S. MAGANA-LOAIZA, M. N. O'SULLIVAN, B. RUDENBURG, M. MALIK, M. P. J. LAVERY, M. J.PADGETT, D. J. GAUTHIER, and R. W. BOYD, *High-dimensional quantum cryptography with twisted light*, New Journal of Physics **17**(3), 2015, paper 033033.

[6] Ş. SUCIU, G. A. BULZAN, T.-A. ISDRAILă, A. M. PăLICI, S. ATAMAN, C. KUSKO and R. IONICIOIU, *Quantum communication networks with optical vortices*, Physical Review A **108**, 2023, paper 052612.

[7] G. GIBSON, J. COURTIAL, M. PADGETT, M. VASNETSOV, V. PAS'KO, S. BARNETT and S. FRANKE-ARNOLD, *Freespace information transfer using light beams carrying orbital angular momentum,* Optics Express **12**(22), 2004, pp. 5448–5456.

[8] J. LEACH, M. J. PADGETT, S. M. BARNETT, S. FRANKE-ARNOLD and J. COURTIAL, *Measuring the orbital angular momentum of a single photon*, Physical Review Letters **88**, 2002, paper 257901.

[9] R. IONICIOIU, *Sorting quantum systems efficiently*, Scientific Reports **6**, 2016, paper 25356.

[10] M. N. O'SULLIVAN, M. MIRHOSSEINI, M. MALIK and R. W. BOYD, *Near-perfect sorting of orbital angular momentum and angular position states of light*, Optics Express **20**, 2012, paper 24444.

[11] G. BERKHOUT, M. LAVERY, J. COURTIAL, M. BEIJERSBERGEN and M. PADGETT, *Efficient sorting of orbital angular momentum states of light*, Physical Review Letters **105**, 2010, paper 153601.

[12] M. P. J. LAVERY, D. J. ROBERTSON, G. G. BERKHOUT, G. D. LOVE, M. J. PADGETT and J. COURTIAL, *Refractive elements for the measurement of the orbital angular momentum of a single photon*, Optics Express **20**, 2012, paper 2110.

[13] M. MIRHOSSEINI, M. MALIK, Z. SHI and R. W. BOYD, *Efficient separation of the orbital angular momentum eigenstates of light*, Nature Communications **4**, 2013, paper 2781.

[14] G. RUFFATO and H. KOBAYASHI, *Roulette caustics in transformation optics of structured light beams*, Optics Communications **490**, 2021, paper 126893.

[15] S. FRANKE-ARNOLD, J. LEACH, M. J. PADGETT, V. E. LEMBESSIS, D. ELLINAS, A. J. WRIGHT, J. M. GIRKIN, P. OHBERG and A. S. ARNOLD, *Optical ferris wheel for ultracold atoms*, Optics Express **15**, 2007, pp. 8619–8625.

[16] G. BULZAN, R. REBIGAN, M. KUSKO, R. TUDOR and C. KUSKO, *Diffractive optical element realizing a logarithmic – polar transformation*, Proceedings of 47$^{\text{th}}$ International Semiconductor Conference, Sinaia, Romania, 2024, pp. 287–290.